ELSEVIER

Journal of Chromatography A, 728 (1996) 25–32

JOURNAL OF CHROMATOGRAPHY A

Steady-state concentration boundary profile for the injection of a single-component feed in counter-current chromatography

Guoming Zhong[a,b], Georges Guiochon[a,b,*]

[a]*Department of Chemistry, University of Tennessee, Knoxville, TN, 37996-1600, USA*

[b]*Division of Chemical and Analytical Sciences, Oak Ridge National Laboratory, Oak Ridge, TN, 37831-6120, USA*

Abstract

In counter-current chromatography, the concentration profile of a single component feed has a steady diffuse boundary located at the opposite side of the shock layer from the feed point. The properties of this feature, unusual in chromatography, are discussed. An analytical solution for the profile of this boundary is derived. It is valid in the case of fast mass transfer kinetics. It explains clearly the formation and stability of this steady-state concentration profile and the influence on its width of axial dispersion and the mass transfer kinetics. Numerical calculations of this steady-state profile were also carried out for the sake of comparison. The results of this study suggest that a similar phenomenon may take place in simulated moving bed operation. They improve our understanding of the counter-current moving bed and simulated moving bed processes in chromatography.

Keywords: Counter-current chromatography; Concentration profile; Axial dispersion; Mass transfer kinetics; Shock layer

1. Introduction

In two previous publications, we have discussed the ideal model solution of counter-current chromatography [1] and the profiles of the shock layers which replace in actual columns the concentration shocks predicted by the ideal model [2]. The latter study allowed the determination of the optimum liquid- and solid-phase velocities in counter-current liquid chromatography [2]. In this work, we pointed out that, when a shock layer is formed in the column, it may move either in the direction of the liquid phase (when the solid-phase velocity is low or moderate), or in the direction of the solid phase (if the solid phase is fast enough). At the opposite end of the band from the shock layer, there is a steady diffuse concentration profile, whose location and profile depends on a balance between apparent axial dispersion, and the velocities of the counter-current liquid and solid phases. This diffuse profile originates ($C=0$) in a point of fixed position. This point and the shock layers are located on the opposite sides of the feed point [2].

The shape of this steady diffuse concentration profile was not investigated in our previous work. It is important to do so, however, for a better understanding of the separation processes in counter-current chromatography and in the simulated moving bed chromatograph. The existence of this steady profile and its properties are useful to know to develop applications of this new preparative technique. Finally, there are not many examples of

* Corresponding author. Address for correspondence: Department of Chemistry, University of Tennessee, Knoxville, TN, 37996-1600, USA.

0021-9673/96/$15.00
SSDI 0021-9673(95)01205-2

steady-state zones in chromatography [3] and this is an interesting example.

The aim of the present work is the study of the shape of this steady diffuse profile, the derivation of an analytical solution in the case of fast mass transfer kinetics, the illustration, and the discussion of this solution which shows clearly the mechanism of formation of this steady-state concentration profile.

2. Theory

This work is a continuation of previous investigations on counter-current liquid chromatography [1,2], in which the mathematical model of this implementation has been discussed in detail. Accordingly, only a brief description of the model is given here.

2.1. The model of steady-state counter-current liquid chromatography

We consider the same counter-current liquid chromatography system as in [1]. Through this entire work, unless otherwise specified, we assume that the equilibrium isotherm is accounted for by the Langmuir model. The feed point is at the center of the column. When the solid-phase velocity is sufficiently low and $1-\beta Fa>0$ (where β=the ratio of the solid to the liquid phase velocities; F=the phase ratio; a=the initial slope of the equilibrium isotherm), the sample moves in the direction of the liquid phase. The profile of the front of the band is a diffuse concentration profile for a linear isotherm. It becomes a shock layer with a constant pattern for a Langmuir isotherm. This front propagates along the positive part of the column, from the central feed point ($x>0$, $x=z/L$, fractional column length).

However, because of the apparent axial dispersion and because the saturated solid phase moves at feed point in the direction opposite to that of the liquid phase, a portion of the sample moves in the direction of the solid phase, toward the other side of the feed point. This portion tends to propagate at counter-current of the incoming solvent. There will be a steady-state, dynamic equilibrium between these forces, the resultant of the velocity contribution of the two phases and axial dispersion. The opposite situation takes place when the solid-phase velocity is high [2]. In this case, a shock layer or a diffuse concentration profile migrates backward, along the negative part of the column toward the solid-phase exit, depending on the nature of the isotherm (Langmuirian or anti-Langmuirian, while a steady-state concentration profile forms at the beginning of the positive side of the column. By contrast with our previous publication [2], we are only interested here in this steady concentration profile.

The system of equations of counter-current liquid chromatography under steady-state can be written under dimensionless form as in our previous papers [1,2]:

$$\frac{\partial C}{\partial x}-\beta F\frac{\partial q}{\partial x}-\frac{1}{Pe}\frac{\partial^2 C}{\partial x^2}=0 \tag{1}$$

$$-\beta\frac{\partial q}{\partial x}=St(f(C)-q) \tag{2}$$

$$f(C)=\frac{aC}{1+bC} \tag{3}$$

with the dimensionless parameters

$$\tau=ut/L,\ x=z/L \tag{4a}$$

$$\beta=v/u,\ Pe=\frac{uL}{D_L},\ St=\frac{kL}{u} \tag{4b}$$

where C and q are liquid and solid-phase concentration, respectively, Pe and St are the Peclet and Stanton number, respectively, L is the column length, u and v are the liquid and solid-phase velocity, respectively, D_L is the axial dispersion coefficient, t, z, and $x=z/L$ ($-1<x<1$) are the time, the axial position, and the dimensionless axial position, respectively. a and b are the numerical coefficients of the Langmuir isotherm ($f(C)$, Eq. 3). When $b=0$, we obtain the linear or Henry's law isotherm. Because we consider a steady-state profile, there is no kinetic equation, the concentrations are constant at any x in the corresponding range around $x=0$, and $\partial q/\partial t=0$.

The boundary and initial conditions of the system of Eqs. 1–3 are:

$$C(x,\tau=0)=0,\ C(0,\tau>0)=C_0,$$
$$q(0,\tau>0)=f(C_0) \tag{5}$$

They correspond to a step injection at the center ($x=0$) of the chromatographic column. It is worth noting that the boundary condition for q is used only for the numerical calculations, but is not useful in the steady-state analysis because of the assumption made that the mass transfer kinetics are fast (see below Eq. 6).

2.2. Steady state analysis

When the mass transfer kinetics are fast, St has a large value and q approaches closely, its equilibrium value, $f(C)$. In such a case, the last term of Eq. 2 can be replaced by the derivative of $f(C)$ and this equation can be rewritten as follows

$$q = f(C) + \frac{\beta}{St}\frac{\partial q}{\partial x} \approx f(C) + \frac{\beta}{St}\frac{\partial f(C)}{\partial x} \tag{6}$$

Eq. 1 can be integrated once by respect to x, which gives

$$C - \beta F q - \frac{1}{Pe}\frac{\partial C}{\partial x} = J_0 \tag{7}$$

where J_0 is the constant mass flow, which can be determined from the boundary condition at the feed point. As steady-state is approached, the mass flow across any section of the column from the feed point to the end of the steady concentration profile tends toward zero. At steady-state, $J_0=0$.

Combination of Eq. 6 and Eq. 7 under steady-state conditions leads to

$$\frac{d\left[\frac{C}{Pe} + \frac{\beta^2 F f(C)}{St}\right]}{C - \beta F f(C)} = \mathrm{d}x \tag{8}$$

In this equation, x may be positive or negative, depending on which side of the column the steady concentration profile is formed. When the solid-phase velocity, β, is small, $C-\beta Ff(C)>0$ and, as explained above, a steady-state concentration profile is formed on the negative side of the column ($x<0$), close to the feed point. When the solid-phase velocity β is large enough and $C-\beta Ff(C)<0$, the steady-state concentration is formed on the positive side of the column ($x>0$). To summarize, the position of the steady-state profile is such that the inequality $(C-\beta Ff(C))x<0$ is always valid. Furthermore, Eq. 7 gives a profile which is symmetrical by respect to x, which means that the steady-state concentration profiles obtained under conditions in which $C-\beta Ff(C)$ is either positive or negative are symmetrical by respect to the feed point.

Using the condition at the feed point, i.e., $x=0$, $C=C_0$, Eq. 7 can be integrated provided that an explicit equation is available for the equilibrium isotherm. Two important particular solutions are discussed.

Linear isotherm

When the isotherm is linear, $b=0$, Eq. 8 can be easily integrated and

$$C = C_0 \exp\left[\frac{(1-\beta Fa)x}{A}\right] \tag{9}$$

with $(1-\beta Fa)x<0$ and $A=1/Pe+\beta^2 Fa/St$.

This solution shows that the steady concentration profile is an exponential profile in the case of a linear isotherm. More particularly, it is a vertical line when $(1-\beta Fa)=0$.

Nonlinear Langmuir isotherm

In this case, integration of Eq. 8 gives

$$\frac{\beta}{St}\ln\left(\frac{1+bC}{1+bC_0}\right) + \frac{A}{1-\beta Fa}\ln\left[\frac{C(bC_0+1-Fa\beta)}{C_0(bC+1-Fa\beta)}\right] = x \tag{10}$$

with $(1-\beta Fa)x<0$ and $A=1/Pe+\beta^2 Fa/St$. This equation simplifies in the particular case for which $(1-\beta Fa)=0$. We obtain

$$\frac{\beta}{St}\ln\left(\frac{1+bC}{1+bC_0}\right) = x + \frac{A}{b}\frac{C_0-C}{C_0 C} \tag{11}$$

3. Illustrations and discussion

Since the analytical solutions obtained, i.e., Eq. 9 and Eq. 10, are symmetrical by respect to x, depending on the sign of $(1-\beta Fa)$, as discussed above, the following discussion can be limited to the case for which $(1-\beta Fa)>0$ and $x<0$. The same steady-state profile, but located on the opposite side of the column (i.e., $x>0$) will be obtained in the opposite

case $(1-\beta Fa<0)$. For a given compound and a given chromatographic system, the only difference between the profiles corresponding to forward and backward propagation is in the moving front. Assuming a Langmuir isotherm, this front is a shock layer in the case of forward migration and a diffuse boundary in case of backward migration. The exact shape of these profiles was discussed in our previous work [1,2] and equations given to account for them. Here we are only interested in the steady profiles.

The numerical results calculated and used for the illustrations presented below were obtained using the nonsteady kinetic model (time model) of countercurrent chromatography discussed in our previous paper [2]. The use of a nonsteady model allows the calculation of some concentration profiles and the illustration of their propagation, showing how the steady-state regimen of the diffuse boundary profiles can be reached, and allowing comparisons with the analytical solution derived above, in this work, using the steady-state model. The following values of the parameters were used for these illustrations, Langmuir isotherm parameters, $a=2.0$ and $b=0.02$ ml/mg, phase ratio, $F=0.25$, i.e., $k_0'=0.5$.

3.1. Linear isotherm ($b=0$)

Because the isotherm is linear, there is no shock layer in this case. The profile of front moving in the direction of the mobile phase is diffuse and its profile is given by the classical erf function, as for a breakthrough curve under linear conditions.

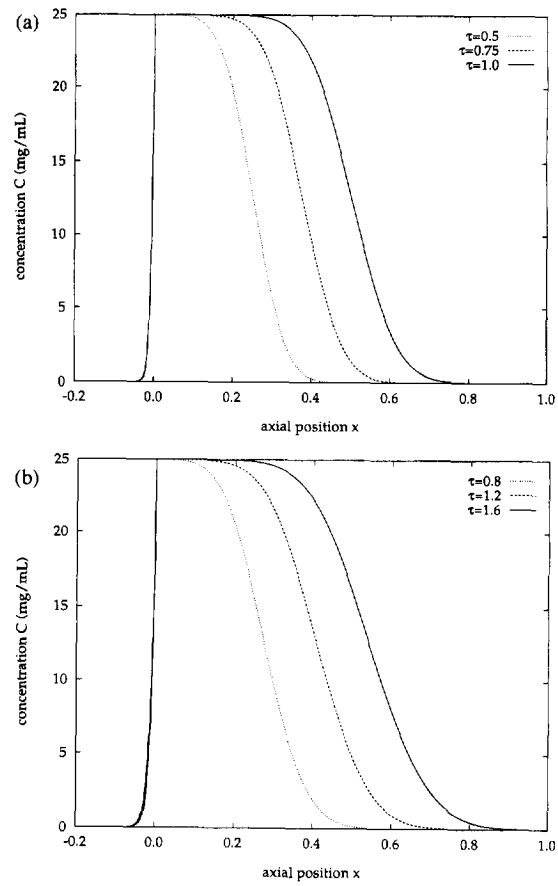

Fig. 1. Linear isotherm. Results of the numerical calculation of the steady-state and propagation profiles. $Pe=200$, $St=1000$. (a) $\beta=0.5$. Profiles calculated for $\tau=0.5$ (dotted line); 0.75 (dashed line); and 1.0 (solid line). (b) $\beta=1.0$. Profiles calculated for $\tau=0.8$ (dotted line); 1.2 (dashed line) and 1.6 (solid line).

Numerical solutions for the steady-state and propagation profiles

Fig. 1a shows three steady-state, axial concentration profiles, obtained as numerical solutions of the nonsteady-state model, for $\beta=0.5$, on the negative side of the column ($x<0$), at three different dimensionless times, $\tau=0.5$ (dotted line), 0.75 (dashed line), and 1.0 (solid line). All three curves are exactly overlaid and cannot be distinguished. This confirms that these axial concentration profiles are steady-state profiles and that they do not change while time is passing.

The corresponding axial concentration profiles on the opposite side (i.e., positive) of the column from the feed point are also plotted in Fig. 1a, to show the concentration distribution in the whole column.

Figure 1b shows similar results, with $\beta=1.0$, at three different times, $\tau=0.8$ (dotted line), 1.2 (dashed line), and 1.6 (solid line). The broadening of the steady-state profile and of the forward moving concentration profile at the three instants selected during its propagation are more intense for this larger value of β.

Comparison between analytical and numerical solutions

The numerical solution of the kinetic (i.e., nonsteady-state) model and the analytical solution of the

steady-state model (i.e., Eq. 9) are compared in Fig. 2. Two different cases are illustrated, corresponding to $\beta=0.5$ (numerical solution, solid line, analytical solution, dashed line) and $\beta=1.0$ (numerical solution, long-dashed line; analytical solution, dotted line). A more diffuse steady-state profile is obtained for the larger value of β because, as predicted by Eq. 9, when $(1-\beta Fa)$ decreases, a larger value of x is needed to achieve the same concentration. Fig. 2 shows that an excellent agreement is obtained between the numerical and the analytical solution. This confirms the validity of the analytical solution.

Effects of the dispersion coefficient and the rate of mass transfer

The analytical solution (Eq. 9) shows that the contributions of the Peclet number and the Stanton number are inversely additive. In other words, the contributions of the axial dispersion and the mass transfer resistance are additive. This property is similar to their additivity in linear and nonlinear (i.e., when a shock layer is formed) chromatography. The only difference with these other cases is in the value of the coefficients of this linear relationship.

As shown by Eq. 9, a larger value of the Peclet number, Pe, or of the Stanton number, St, leads to a sharper steady-state profile. This is illustrated in Fig. 3a. The solid line corresponds to $Pe=1000$ and

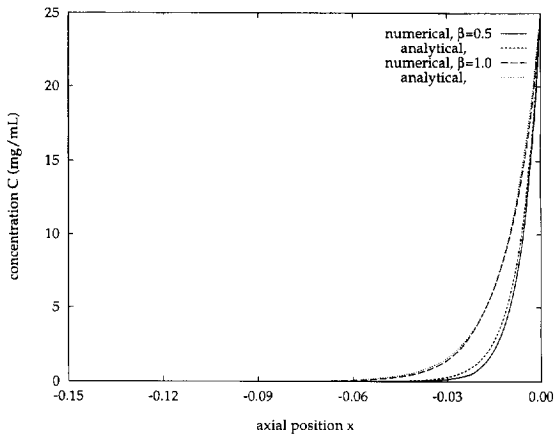

Fig. 2. Linear isotherm. Comparison between the analytical and the numerical solution of the steady-state profile. $Pe=200$, $St=1000$. $\beta=0.5$. Numerical solution, solid line; analytical solution (Eq. 10), dashed line. $\beta=1.0$. Numerical solution, long-dashed line; analytical solution (Eq. 10), dotted line.

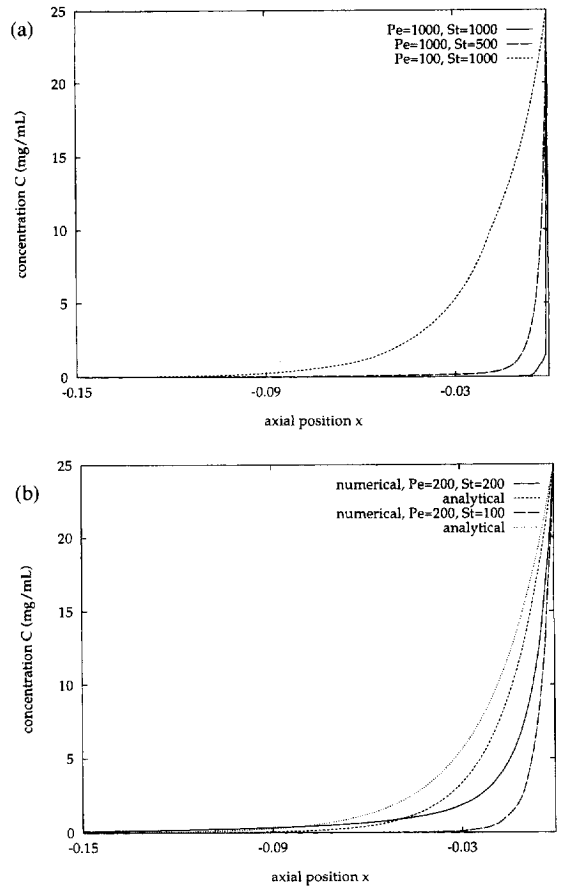

Fig. 3. Linear isotherm. Effects of the axial dispersion and mass transfer resistance. $\beta=1.0$. (a) Solid line, $Pe=1000$ and $St=1000$); long-dashed line, $Pe=1000$ and $St=500$; and dashed line, $Pe=100$ and $St=1000$. (b) $Pe=200$ and $St=200$: numerical, solid line; analytical, dashed line, $Pe=200$ and $St=100$: numerical, long-dashed line; analytical, dotted line.

$St=1000$. It gives a sharper profile than the long-dashed line, corresponding to $Pe=1000$ and $St=500$, while the dashed line, corresponding to $Pe=100$ and $St=1000$, allows for a very diffuse steady-state profile.

The opposite situation is observed, however, at low values of the Stanton number, as illustrated in Fig. 3b. The profiles compared are obtained as results of the numerical calculation for values of the Stanton number which are no longer large enough for the assumption made in writing Eq. 6 to be valid. The solid and long-dashed lines correspond to $St=200$ and 100, respectively. In this case, the larger

Stanton number leads to a more diffuse profile than the smaller one. The reason is that a smaller value of the Stanton number means simultaneously a less strongly adsorbed component and a smaller amount of this component carried by the solid phase into the negative side of the column. Accordingly, a less diffuse steady-state profile is obtained. This is contrary to the prediction of the analytical solution, Eq. 9, represented by the dashed line ($St=200$), less diffuse than the dotted line ($St=100$). The analytical solution is no longer valid, however, as just explained, because the assumption of a large value of St used to write Eq. 6 and derive Eq. 9 is no longer valid.

3.2. Nonlinear isotherm

The front of the forward moving band is now a shock layer provided the concentration step, the axial dispersion coefficient, and the rate of the mass transfer kinetics are sufficiently large.

Numerical steady and propagation profiles

Fig. 4a and Fig. 4b show three series of steady-state (left) and propagation (right) profiles obtained with a Langmuir isotherm for values of the reduced time, τ, of 0.5 (dotted line, 0.75 (dashed line), and 1.0 (solid line), respectively. In all three cases, $\beta=0.5$. Note that in this case ($b=0.02$ ml/mg), the product bC is equal to 0.5, which indicates strong nonlinear behavior. The three steady-state profiles overlay exactly. The three propagation profiles are qualitatively very similar to those in Fig. 1a and Fig. 1b. The difference between these two series of profiles is that, in Fig. 4a and Fig. 4b the isotherm is no longer linear but follows the Langmuir equation. Thus, the front of the forward moving bands in Fig. 4a and Fig. 4b are shock layers. For this reason, they are somewhat steeper than the corresponding ones in Fig. 1a and Fig. 1b, they exhibit constant pattern behavior and propagate at a constant velocity (equal to the shock velocity) along the column without changing shape.

It is striking to observe that, although the profile on the left side of Fig. 4a is much steeper than any of three profiles on the right side, the left profile is a diffuse boundary, albeit a steady-state one, while the right three profiles are shock layers. This is a known

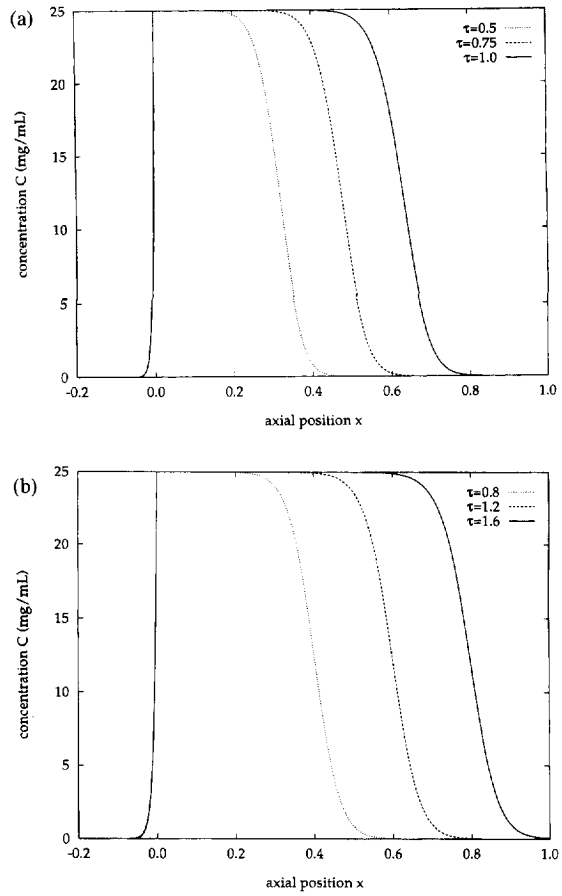

Fig. 4. Langmuir isotherm. Results of the numerical calculation of the steady-state and propagation profiles. $Pe=200$, $St=1000$. (a) $\beta=0.5$. Profiles calculated for $\tau=0.5$ (dotted line); 0.75 (dashed line); and 1.0 (solid line). (b) $\beta=1.0$. Profiles calculated for $\tau=0.8$ (dotted line); 1.2 (dashed line); and 1.6 (solid line).

property of steady-state profiles [3] which, unfortunately, are rare in chromatography.

While there are some visible differences between the propagation profiles in Fig. 1 and Fig. 4, the difference between the steady-state profiles in Fig. 1 and Fig. 4 is too small to be observed here. It will be discussed later.

The profiles shown in Fig. 4b are similar to those in Fig. 4a but a different value of $\beta(1.0)$ is used and the reduced times are $\tau=0.8$ (dotted line), 1.2 (dashed line), and 1.6 (solid line). The main differences with the profiles in Fig. 4a are slightly more

diffuse steady-state and propagation profiles and a different shock velocity.

Comparison between analytical and numerical results

Fig. 5 compares the profiles derived from the analytical solution of the steady-state model (Eq. 10) and those calculated numerically, for two values of β: 0.5 and 1.0. We observe, first, an excellent agreement between the analytical and the numerical results. Second, comparing Fig. 2 and Fig. 5, we see that the steady-state profiles are narrower for the nonlinear isotherm than for the linear one. Finally, as in the case of the linear isotherm (Fig. 2), a more diffuse profile is associated with the larger value of β(β=1.0).

Effects of the dispersion and mass transfer

The results obtained in this investigation are similar to those reported above in the case of a linear isotherm (Fig. 3). They are summarized in Fig. 6a and Fig. 6b. When the Stanton number is relatively large, larger values of the Peclet number or Stanton number lead to sharper profiles. This effect is illustrated in Fig. 6a by the solid line (Pe=500 and St=2000), the long-dashed line (Pe=500, St=1000) and the dashed line (Pe=200, St=1000). However

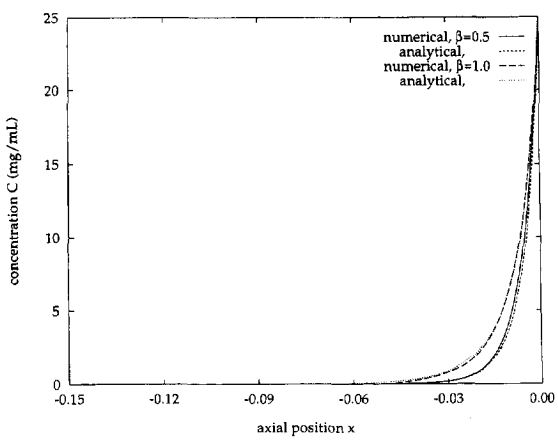

Fig. 5. Langmuir isotherm. Comparison between the analytical and the numerical solution of the steady-state profile. Pe=200, St=1000. β=0.5. Numerical solution, solid line; analytical solution, dashed line. β=1.0. Numerical solution, long-dashed line; analytical solution, dotted line.

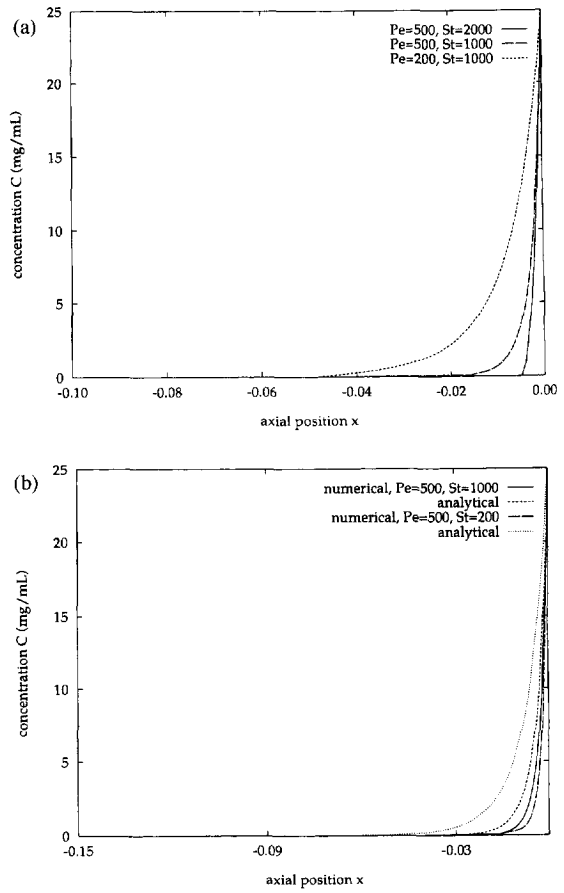

Fig. 6. Langmuir isotherm. Effects of the axial dispersion and mass transfer resistance. β=1.0. (a) Solid line, Pe=500 and St=2000; long-dashed line, Pe=500 and St=1000; and dashed line, Pe=200 and St=1000. (b) Pe=500 and St=1000: numerical, solid line; analytical, dashed line. Pe=500 and St=200: numerical, long-dashed line; analytical, dotted line.

the profiles in Fig. 6b show that, when the Stanton number is not large enough (e.g., St=200, long-dashed line), a smaller Stanton number can give a sharper profile, as calculated with the numerical method (compare long-dashed and solid line). The reason is that a smaller Stanton number means a smaller amount of component adsorbed in the solid phase and a smaller mass brought by the solid phase into the negative side of the column; as a consequence, the steady-state profile is less diffuse than with a somewhat larger Stanton number. This appears to be in contradiction with the prediction of the

analytical solution (Eq. 10). However, this result is explained by the failure of the assumption made earlier that the Stanton number is large. Thus, Eq. 10 is no longer valid, which explains the disagreement between the solutions of the analytical and numerical equations.

4. Glossary of symbols

a, b first and second parameters of the Langmuir isotherm
C liquid phase concentration of the component
D_L axial dispersion coefficient
F phase ratio
k mass transfer coefficient
L column length
Pe Peclet number ($=uL/D_L$)
q solid-phase concentration
St Stanton number ($=kL/u$)
t time
u liquid phase flow velocity
v solid-phase flow velocity
x dimensionless axial position in the column ($=z/L$)
z axial position in the column

4.1. Greek symbols

β ratio of the solid- and liquid-phase velocity ($=v/u$)
τ dimensionless time ($=ut/L$)

Acknowledgments

This work has been supported in part by Grant CHE-9201663 of the National Science Foundation and by the cooperative agreement between the University of Tennessee and the Oak Ridge National Laboratory. We acknowledge support of our computational effort by the University of Tennessee Computing Center.

References

[1] G.M. Zhong and G. Guiochon, J. Chromatogr. A, 688 (1994) 1.
[2] G.M. Zhong and G. Guiochon, J. Chromatogr. in press.
[3] J.C. Giddings, Unified Separation Science, Wiley, New York, 1991.